https://doi.org/10.2352/ISSN.2470-1173.2017.13.IPAS-200

2-D Octonion Discrete Fourier Transform: Fast Algorithms

In color imaging, the two-dimension discrete Fourier transform (2-D DFT) is used to process separately color channels and in the quaternion space the processing of the image with 2-D quaternion Fourier transforms do consider interactions between the color channels. The color image can be also considered in different models with transformation to the octonion space with following processing in the 8-D frequency domain. In this work, we describe the algorithm for the 2-D two-side octonion DFT (ODFT), by using two-side 2-D quaternion DFTs.

1. Introduction

There were many attempts to generalize the known concept of the 2-D DFT, including the 2-D quaternion discrete Fourier transform tailored to color images [1]-[5]. The two-sided quaternion discrete Fourier transformation (QDFT) was introduced to analyze the 2-D linear time-invariant partial-differential systems [6]. The classical fast algorithms are based on representation of the QDFT by a combinations of a few classical DFT transforms [7]. This allows us to obtain QDFT fast numerical implementation with the standard FFT algorithms [15]-[18].

In this paper, we describe the concept of the two-side 2-D octonion DFT (ODFT) and present its algorithm. The calculation of the transform is reduced to calculation of two 2-D QDFT which has fast algorithms [1, 7]-[9]. The octonion algebra with the Fourier transform can be used in color imaging as the 2-D ODFT, which found effective applications in color imaging [20, 24], medical imaging [21]-[23], in image filtration [1, 42], image enhancement [25, 37]-[41],. The octonion 2-D DFT can be used not only in color imaging, but in gray-scale imaging as well, and for that there are many models of transferring one or a few gray-scale images into the octonion space.

2. Octonion and Images

It is known that the number of imaginary components that could be added to the real numbers to define new arithmetics with operations of addition, multiplication and division can be only 1, 3, and 7. The first two cases relate to the complex and quaternion numbers [10], respectively. In this paper, we consider the arithmetic of numbers with seven-component imaginary part, which generalize the quaternion numbers and allow for adding, multiplying and dividing the numbers [1, 11, 12]. These numbers are called octonions or Cayley numbers and were discovered independently by the Irish mathematician John Graves (1806–1870) and the English mathematician Arthur Cayley (1821-1895).

The quaternion numbers q were introduced as numbers from the doubled complex plane C^2, which are defined as $q = z_1 + jz_2 = (x_1 + iy_1) + j(x_2 + iy_2) = x_1 + iy_1 + jx_2 + (ji)y_2$. The quaternions also can be defined as $q = z_1 + z_2 j = (x_1 + iy_1) + (x_2 + iy_2)j = x_1 + iy_1 + jx_2 + (ij)y_2$, where the product (ij) is denoted by k. The quaternion are four-dimensional generation of a complex number with one real part and three component imaginary part. The imaginary dimensions are represented as i, j, and k. Any quaternion q may be represented in a hyper-complex form as $q = a + bi + cj + dk = a + (bi + cj + dk)$, where a, b, c, and d are real numbers and i, j, and k are three imaginary units with multiplication laws:

$$ij = -ji = k, \quad jk = -kj = i,$$
$$ki = -ik = -j, \quad i^2 = j^2 = k^2 = ijk = -1.$$

The number a is considered to be the real part of q and $(bi + cj + dk)$ is the "imaginary" part of q. The quaternion conjugate and modulus of q equal

$$\bar{q} = a - (bi + cj + dk), \quad |q| = \sqrt{a^2 + b^2 + c^2 + d^2},$$

respectively. The property of commutativity does not hold in quaternion algebra, i.e., there are many quaternions $q_1 \neq q_2$, such that $q_1 q_2 \neq q_2 q_1$.

A $(2,2)$-representation was applied to quaternions and new numbers defined, which first were called "double-quaternions," or "octives" by John Graves and then "octonions" [12]. The arithmetic with octonions includes the operations of addition, multiplication, and division. Let $q_1 = a_1 + q_1'$ and $q_2 = a_2 + q_2'$ be quaternion numbers, and let o be the double-quaternion, i.e., the number of type

$$o = (q_1, q_2) = q_1 + q_2 E = (a_1 + q_1') + (a_2 + q_2')E, \qquad (1)$$

where E is a symbol to be defined for a unit which commutates with the real numbers. Considering the imaginary parts of the quaternions, $q_1' = ib_1 + jc_1 + kd_1$ and $q_2' = ib_2 + jc_2 + kd_2$, we obtain the octonion number with the eight component number $o = (a_1, b_1, c_1, d_1, a_2, b_2, c_2, d_2) = a_1 + ib_1 + jc_1 + kd_1 + a_2 E + Ib_2 + Jc_2 + Kd_2$. Thus, we can write octonions in the form of

$$o = a + ib + jc + kd + AE + IB + JC + KD, \qquad (2)$$

where a, b, c, d and A, B, C, D are real numbers. Here, we denote the numbers iE, jE, kE by I, J, and K, respectively. The first component, a, is considered to be the real part of the octonion, and the remaining seven components together compose the "imaginary" part of o. The operation of addition of octonions $o_1 = q_1 + q_2 E$ and $o_2 = r_1 + r_2 E$, is performed component-wise,

$$o_1 + o_2 = (q_1 + q_2 E) + (r_1 + r_2 E) = (q_1 + r_1) + (q_2 + r_2)E.$$

The conjugate of the octonion $o = q_1 + q_2 E$ is defined as

$$\begin{aligned} \bar{o} &= a - (ib + jc + kd + AE + IB + JC + KD) \\ &= (a - ib - jc - kd) - (AE + IB + JC + KD) \\ &= \bar{q}_1 - q_2 E. \end{aligned} \qquad (3)$$

All seven numbers i, j, k, E, I, J, K are called *imaginary units.*

1. The multiplication of two octonions $o_1 = q_1 + q_2E$ and $o_2 = r_1 + r_2E$, which is defined as

$$o_1 o_2 = (q_1 r_1 - \bar{r}_2 q_2) + (r_2 q_1 + q_2 \bar{r}_1)E, \tag{4}$$

to preserve the multiplication of quaternion numbers and to satisfy the property $|o_1 o_2|^2 = |o_1|^2 |o_2|^2$. The module o_1 of the octonion $o_1 = q_1 + q_2E$ is calculated by $\sqrt{o_1 \bar{o}_1}$ and equals

$$\begin{aligned} o_1\bar{o}_1 &= (q_1+q_2E)(\bar{q}_1 - q_2E) + = (q_1\bar{q}_1 + \bar{q}_2 q_2) \\ &\quad +(-q_2q_1 + q_2q_1)E = |q_1|^2 + |q_2|^2 \\ &= (a_1^2+b_1^2+c_1^2+d_1^2) + (a_2^2+b_2^2+c_2^2+d_2^2) \\ &= (a_1^2+b_1^2+c_1^2+d_1^2) + (A_1^2+B_1^2+C_1^2+D_1^2). \end{aligned} \tag{5}$$

Therefore, $\bar{o}_1 o_1 = |q_1|^2 + |q_2|^2 = o_1\bar{o}_1$.

The basic multiplications of imaginary units and the real number 1 are shown in Table 1.

	1	i	j	k	E	I	J	K
1	1	i	j	k	E	I	J	K
i	i	1	k	j	I	E	K	J
j	j	k	1	i	J	K	E	I
k	k	j	i	1	K	J	I	E
E	E	I	J	K	1	i	j	k
I	I	E	K	J	i	1	k	j
J	J	K	E	I	j	k	1	i
K	K	J	I	E	k	j	i	1

Table 1. Multiplication rules of the octonion unit numbers

Example 1 Consider two octonions

$$\begin{aligned} o_1 &= 1+2i-3j+4k+E+2I+3J-K, \\ o_2 &= 2-i+2j+2k-3E+4I+J+2K. \end{aligned}$$

The multiplication of these octonions equals $o_1 o_2 = 2+8j+24k-8E+7I+J-39K$. For comparison, $o_2 o_1$ equals

$$o_2 o_1 = 2+6i-16j-4k+14E+9I+13J+39K \neq o_1 o_2.$$

Since $E^2 = I^2 = J^2 = K^2 = -1$, we obtain the following:

$$|o|^2 = a^2+b^2+c^2+d^2+E^2+I^2+J^2+K^2. \tag{6}$$

For example, for the octonion $o = 1+2i-3J-4K$, the square of its module $|o|^2 = 1+2^2+3^2+4^2 = 30$. The multiplication of octonions is not associative, i.e., not for all octonions o_1, o_2, and o_3, the equality $(o_1 o_2)o_3 = o_1(o_2 o_3)$ holds.

Consider the square of the octonion $o = q_1 + q_2E$, where $q_1 = a_1 + q_1'$ and $q_2 = a_2 + q_2'$. As directly follows from (5), the square of the octonion, $o^2 = oo$, can be written as

$$o^2 = -(a_1^2+a_2^2) - \left(|q_1'|^2 + |q_2'|^2\right) + 2a_1 o = -|o|^2 + 2a_1 o.$$

If we consider that $o = a_1 + o'$, where the imaginary part of the octonion is $o' = q_1' + q_2E$, then the square of the octonion can be written as

$$\begin{aligned} o^2 &= 2a_1 o - |o|^2 = 2a_1(a_1+o') - \left(a_1^2 + |o'|^2\right) \\ &= a_1^2 - |o'|^2 + 2a_1 o'. \end{aligned} \tag{7}$$

If the octonion is pure imaginary, i.e., $a_1 = 0$, then the square $o^2 = -|o'|^2$ is a negative number.

When the octonion $o = a_1 + o'$ is unit, i.e., $|o|^2 = 1$, and its square $o^2 = -1$, then it follows from (7) that the following holds: $a_1^2 - |o'|^2 + 2a_1 o' = -1$. This equality can be solved only when $2a_1 o' = 0$, which means that $a_1 = 0$ and therefore $o = o'$. Then, $|o|^2 = 1$ and $o^2 = -1$, i.e., the octonion is a unit pure octonion (with its real part equals zero). The examples of pure unit octonions are i, j, k, E, I, J, K, and

$$o_1 = \frac{i+j+k+E+I+J+2K}{\sqrt{10}}, \quad o_2 = \frac{i+j-2I+J}{7}.$$

We consider the exponential function and representation of octonions in a polar form.

2. The exponential function on octonions o is defined by the Taylor series as

$$e^o = \exp(o) = 1 + \sum_{n=1}^{\infty} \frac{o^n}{n!}. \tag{8}$$

Now, we consider a pure unit octonion which we denote by

$$\lambda = \lambda' = i\lambda_i + j\lambda_j + k\lambda_k + E\lambda_E + I\lambda_I + J\lambda_J + K\lambda_K.$$

Let ϑ be the real number which stands for the variable angle. Since $\lambda^2 = -1$, by using the Taylor series, we can define the exponential function as

$$\exp(\lambda\vartheta) = \cos(\vartheta) + \lambda\sin(\vartheta). \tag{9}$$

The conjugate octonion exponential function is $\exp(-\lambda\vartheta) = \cos(\vartheta) - \lambda\sin(\vartheta)$.

The octonion o can be written as $o = a + \lambda\vartheta$, where the λ is a pure octonion and ϑ is a real number. Therefore we can write the following general formula for the octonion exponential function:

$$e^o = e^{a+\lambda\vartheta} = e^a e^{\lambda\vartheta} = e^a(\cos(\vartheta) + \lambda\sin(\vartheta)). \tag{10}$$

Example 2 Consider the octonion $o = 1+i-2j+k+2E+I-J+2K$ which can be written as

$$o = 1 + \lambda\vartheta = 1 + \frac{i-2j+k+2E+I-J+2K}{4}4.$$

For this octonion, $a = 2$ and the angle

$$\vartheta = |o'| = \sqrt{1+2^2+1+2^2+1+1+2^2} = \sqrt{16} = 4,$$

and the pure unit octonion

$$\lambda = \frac{i-2j+k+2E+I-J+2K}{4}.$$

The exponential number $\exp(o)$ is calculated by

$$e^o = e^1\left(\cos(4) + \frac{i-2j+k+2E+I-J+2K}{4}\sin(4)\right).$$

Denoting by $C = e/4 \approx 0.6796$, we can write the octonion exponent as $e^o = e^1\cos(4) + C\sin(4)(i-2j+k+2E+I-J+2K)$.

3. Color-to-Octonion Images

A discrete color image $f_{n,m}$ in the RGB color space can be transformed into imaginary part of quaternion numbers form by encoding the red, green, and blue components of the RGB value as a pure quaternion (with zero real part): $f_{n,m} = 0 + (ir_{n,m} + jg_{n,m} + kb_{n,m})$. In quaternion imaging, each color triple is treated as a whole unit [2], and it thus is expected, that by using quaternion operations, a higher color information accuracy can be achieved. The zero real part of the quaternion image makes it pure quaternion, and we could use the gray-scale component in the real part

$$\begin{aligned} f_{n,m} &= a_{n,m} + (ir_{n,m} + jg_{n,m} + kb_{n,m}) \\ &= \tfrac{r_{n,m}+g_{n,m}+b_{n,m}}{3} + (ir_{n,m} + jg_{n,m} + kb_{n,m}). \end{aligned} \tag{11}$$

When using the CMYK color model [2, 14], with the primary colors cyan (C), magenta (M), yellow (Y), the quaternion image is four-component image with the real part equal the black (K) color, $f_{n,m} = k_{n,m} + (ic_{n,m} + jm_{n,m} + ky_{n,m})$.

There are different ways to compose or transfer color images into the octonion space and then introduce the concept of the octonion image. We consider one of such ways, by using the RGB color model. Let $N \times M$ be the size of the $f_{n,m}$ image components, i.e., $n = 0 : (N-1)$ and $m = 0 : (M-1)$, and let N and M be even numbers. We consider that the image is the color image transformed to the quaternion space as shown in (11). This quaternion image with four components can be transformed to the octonion space, by composing the following "octonion image":

$$\begin{aligned} o_{n,m} &= f_{n,m} + f_{n+1,m}E \\ &= a_{n,m} + ir_{n,m} + jg_{n,m} + kb_{n,m} + \\ &\quad + Ea_{n+1,m} + Ir_{n+1,m} + Jg_{n+1,m} + Kb_{n+1,m}, \end{aligned} \tag{12}$$

where $n = 0 : (N/2-1)$, $m = 0 : (M-1)$. The octonion image $o_{n,m} = (f_{n,m}, f_{n+1,m})$ is of size $(N/2) \times M$. We also can consider the "octonion image" with the following composition:

$$\begin{aligned} o_{n,m} &= f_{n,m} + f_{n,m+1}E \\ &= a_{n,m} + ir_{n,m} + jg_{n,m} + kb_{n,m} \\ &\quad + Ea_{n,m+1} + Ir_{n,m+1} + Jg_{n,m+1} + Kb_{n,m+1}. \end{aligned} \tag{13}$$

The octonion image $o_{n,m} = (f_{n,m}, f_{n,m+1})$ is of size $N \times (M/2)$.

As an example, Figure 1 shows the color image $(r_{n,m}, g_{n,m}, b_{n,m})$ of size 256×256 in part a. The octonion image $o_{n,m}$ with components of size 128×512 each was calculated by (12). Three i, j, and k-components of $o_{n,m}$ as one color image in the RGB model together with the color image composed by the I, J, and K-components of $o_{n,m}$ are shown in part b.

Figure 2 shows the gray-scale image $a_{n,m}$ of size 256×256 in part a, and the real part and E-component of the octonion image together in part b. Thus, the 256×256 color "tree" image of the RGB model is presented as the "octonion" image with its eight components of size 128×256 each, as shown in Figure 3. The gray-scale image $a_{n,m}$ of the color image, which is the real component of the octonion image $o_{n,m}$ is shown in part a. The three components, i.e., the (i, j, k)-part of the imaginary part of the octonion image $o_{n,m}$ is shown in b, as the color image in the RGB model. In part c, the imaginary E-components of $o_{n,m}$ is shown, as a gray-scale image. The color image in d represents the (I, J, K)-part of the imaginary part of the octonion image $o_{n,m}$. The images in part a and b represent the first quaternion image $q_{n,m}$ and two

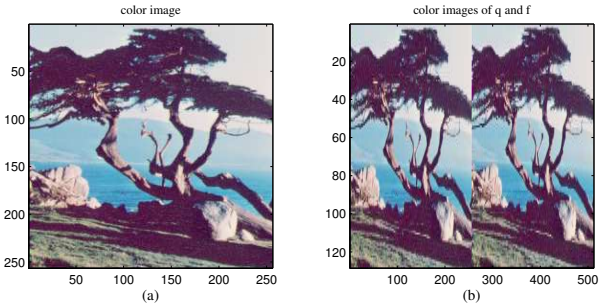

Figure 1. (a) The color "tree" image and (b) the (i, j, k) and (I, J, K) color images.

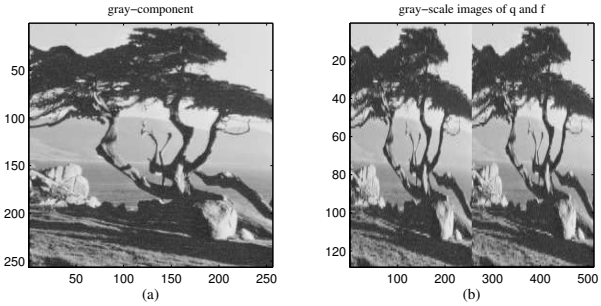

Figure 2. (a) The gray-scale image $a_{n,m}$ and (b) E-components of the octonion "tree" image.

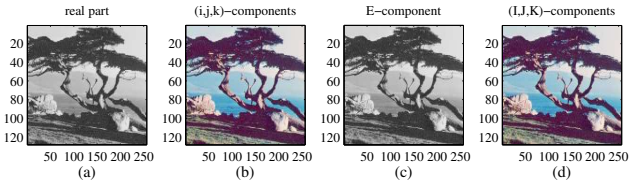

Figure 3. (a) The gray-scale component, (b) the (i, j, k)-component color image, (c) the E-component, and (d) the (I, J, K)-component color image of the octonion "tree" image.

images in parts c and d represent the second quaternion image $f_{n,m}$ of the octonion image $o_{n,m}$. The 256×256 color "tree" image has been transferred to the 128×256 octonion image.

In the similar way, the 362×500 "flowers" image can be transferred to the 181×500 octonion image, as shown in Figure 4.

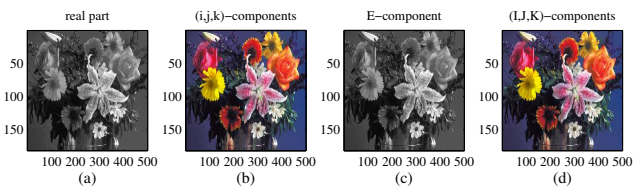

Figure 4. (a) The gray-scale components, (b) the (i, j, k)-component color image, (c) the E-component, and (d) the (I, J, K)-component color image of the octonion "flowers" image.

The color image can also be divided by two halves, and each halve can be transformed to the quaternion space and two quater-

nion images $q_{n,m}$ and $f_{n,m}$ are composed, which together result in a octonion image. In this simple model, two parts q and f are not much correlated, in comparison to the model described above. If we have a sequence of color images or gray-scale images, by taking a few such images new octonion images can be composed. For instance, eight gray-scale images of the same size each can be united in one octonion image, and two color images can be united in one octonion image. The gray-scale image also can be divided by eight parts of size $(N/4)\times(M/2)$ or $(N/2)\times(M/4)$ and considered as components of the octonion image.

4. Two-side 2-D octonion DFT

The octonion discrete Fourier transform (ODFT) is a new concept which allows for processing a few gray-scale or color images, as well as images with their local information as one octonion 8-D image in the spectral domain. This concept generalizes the traditional complex and quaternion 2-D DFTs and can be effectively used for parallel processing up to eight of gray-scale images or two color images. We consider the two-side 2-D ODFT of the octonion image of size $N\times M$. The octonion numbers are dual quaternions, i.e., any octonion o is represented by q_1+q_2E, where q_1 and q_2 are quaternions. The 2-D ODFTs can be calculated by the 1-D and 2-D QDFTs (for more detail, see [1]).

Given two pure unit octonions λ_1 and λ_2, which we consider equal to the pure unit quaternions μ_1 and μ_2, the two-side 2-D OQFT of the octonion image $o_{n,m}$ can be defined as

$$\begin{aligned} O_{p,s} &= \sum_{n=0}^{N-1}\sum_{m=0}^{M-1} W_{\mu_1}^{np}\left(o_{n,m}W_{\mu_2}^{ms}\right) \\ &= \sum_{n=0}^{N-1} W_{\mu_1}^{np}\left(\sum_{m=0}^{M-1} o_{n,m}W_{\mu_2}^{ms}\right), \end{aligned} \tag{14}$$

where $p=0:(N-1)$ and $s=0:(M-1)$. The basis functions are defined by the exponential coefficients

$$\begin{aligned} W_{\mu_1} = W_{\mu_1;N} &= \cos(2\pi/N)-\mu_1\sin(2\pi/N), \\ W_{\mu_2} = W_{\mu_2;M} &= \cos(2\pi/M)-\mu_2\sin(2\pi/M). \end{aligned}$$

We denote the kernel of the transform by (W_{μ_1},W_{μ_2}). To calculate the 2-D two-side ODFT, the row-column method can be used. Along each row (when n is fixed) the M-point right-side ODFT is calculated, and then along each column (when m is fixed) of the obtained data, the N-point left-side ODFT is calculated.

One can also apply the 2-D QDFTs to calculate this transform. To show that, we consider the first and second quaternion components of the image $o_{n,m}=q_{n,m}+f_{n,m}E$ and write

$$\begin{aligned} O_{p,s} &= \sum_{n=0}^{N-1} W_{\mu_1}^{np}\left(\sum_{m=0}^{M-1} q_{n,m}W_{\mu_2}^{ms}\right) \\ &\quad + \sum_{n=0}^{N-1} W_{\mu_1}^{np}\left(\sum_{m=0}^{M-1} (f_{n,m}E)W_{\mu_2}^{ms}\right). \end{aligned}$$

It not difficult to show the following property: $(q_{n,m}E)W_{\mu_2}^{ms}=(q_{n,m}W_{\mu_2}^{-ms})E$. Therefore, we obtain

$$\begin{aligned} O_{p,s} &= \sum_{n=0}^{N-1} W_{\mu_1}^{np}\left(\sum_{m=0}^{M-1} q_{n,m}W_{\mu_2}^{ms}\right) \\ &\quad + \sum_{n=0}^{N-1} W_{\mu_1}^{np}\left(\sum_{m=0}^{M-1} f_{n,m}W_{\mu_2}^{-ms}\right)E. \end{aligned}$$

It should be noted, that $W_{\mu_2}^{-ms}=W_{\mu_2}^{m(M-s)}=W_{-\mu_2}^{ms}$.

Thus, to calculate the two-side 2-D ODFT, we can perform the two-side 2-D QDFT of the quaternion image $q_{n,m}$ and the two-side 2-D QDFT of the quaternion image $f_{n,m}$. The first two-side QDFT is calculated with the kernel (W_{μ_1},W_{μ_2}), and the second one with the kernel (W_{μ_1},W_{μ_2}), or $(W_{\mu_1},W_{-\mu_2})$. Let $Q_{p,s}$ be the two-side QDFT of the image $q_{n,m}$ and let $F_{p,s}$ be the two-side 2-D QDFT of $f_{n,m}$, with the kernel (W_{μ_1},W_{μ_2}) both. Then,

$$O_{p,s}=Q_{p,s}+F_{p,M-s}E.$$

If $F_{p,s}$ is the two-side 2-D QDFT of $f_{n,m}$, with the kernel $(W_{\mu_1},W_{-\mu_2})$, then $O_{p,s}=Q_{p,s}+F_{p,s}E$.

As an example for the "tree" color image, Figure 5 shows the 2-D QDFT, $Q_{p,s}$, of the image $g_{n,m}$ in part a, and the 2-D QDFT, $F_{p,M-s}$, of the image $f_{n,m}$ in part b. These two 2-D QDFTs define the 2-D ODFT of the octonion image $o_{n,m}$. The magnitude of the

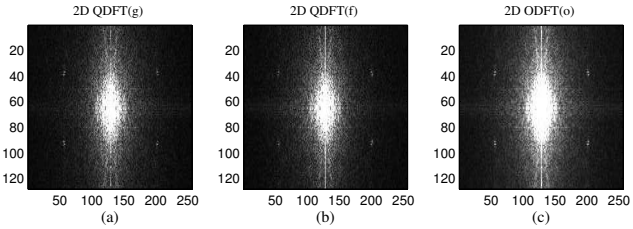

Figure 5. The 2-D QDFT of the quaternion image (a) $g_{n,m}$ and (b) $f_{n,m}$. (c) The 2-D ODFT of the octonion "tree" image $o_{n,m}$.

2-D ODFT of the image $o_{n,m}$ is shown in part c. All transforms are cyclically shifted to the center.

4.1 1-D left-side and right-side QDFTs

We describe briefly the algorithm for calculating the right-side 1-D QDFT [7]. Let $q_n=(a_n,b_n,c_n,d_n)=a_n+ib_n+jc_n+kd_n$ be the quaternion signal of length N. The transform is defined as

$$Q_p=Q_1(p)+iQ_i(p)+jQ_j(p)+kQ_k(p)=\sum_{n=0}^{N-1} q_nW_{\mu}^{np},$$

where $p=0:(N-1)$, and μ is a pure unit quaternion number $\mu=m_1i+m_2j+m_3k$, $\mu^2=-1$. Let φ_{np} be the angle $(2\pi/N)np$. For a real signal x_n of length N, we define the following cosine and sine transforms being the real and imaginary parts of the 1-D DFT of this signal:

$$\begin{aligned} C_x(p) &= \Re(X_p)=\sum_{n=0}^{N-1} x_n\cos(\varphi_{np}), \\ S_x(p) &= \Im(X_p)=\sum_{n=0}^{N-1} x_n\sin(\varphi_{np}), \end{aligned} \tag{15}$$

when $p=0:(N-1)$. Let $C(x)$ and $S(x)$ be the vectors of coefficients $(C_x(0),C_x(1),C_x(2)\ldots,C_x(N-1))$ and $(S_x(0),S_x(1),S_x(2)\ldots,S_x(N-1))$, respectively. The four vectors of coefficients $Q_1(p)$, $Q_i(p)$, $Q_j(p)$, and $Q_k(p)$ are also defined as Q_1, Q_i, Q_j, and Q_k. If we denote the N-point 1-D DFTs of the parts a_n, b_n, c_n, and d_n of the quaternion signal q_n by A_p, B_p, C_p,

and D_p, respectively, we can calculate the 1-D QDFT. The vector $(Q_1(p), Q_i(p), Q_j(p), Q_k(p))'$ in matrix form can be written as

$$\begin{bmatrix} \Re(A_p) \\ \Re(B_p) \\ \Re(C_p) \\ \Re(D_p) \end{bmatrix} + \begin{bmatrix} 0 & m_1 & m_2 & m_3 \\ -m_1 & 0 & -m_3 & m_2 \\ -m_2 & m_3 & 0 & -m_1 \\ -m_3 & -m_2 & m_1 & 0 \end{bmatrix} \begin{bmatrix} \Im(A_p) \\ \Im(B_p) \\ \Im(C_p) \\ \Im(D_p) \end{bmatrix}.$$

Here, $\Re(A)$ and $\Im(A)$ denote the real and imaginary parts of a complex number A, respectively.

The left-side 1-D quaternion DFT (ls-QDFT) is defined as

$$Q_p = Q_1(p) + iQ_i(p) + jQ_j(p) + kQ_k(p) = \sum_{n=0}^{N-1} W_\mu^{np} q_n.$$

The calculation of the transform $(Q_1(p), Q_i(p), Q_j(p), Q_k(p))'$ can be written in matrix form as [1]

$$\begin{bmatrix} \Re(A_p) \\ \Re(B_p) \\ \Re(C_p) \\ \Re(D_p) \end{bmatrix} + \begin{bmatrix} 0 & m_1 & m_2 & m_3 \\ -m_1 & 0 & m_3 & -m_2 \\ -m_2 & -m_3 & 0 & m_1 \\ -m_3 & m_2 & -m_1 & 0 \end{bmatrix} \begin{bmatrix} \Im(A_p) \\ \Im(B_p) \\ \Im(C_p) \\ \Im(D_p) \end{bmatrix}.$$

By using the fast Fourier transforms [17]-[19, 26, 33, 35], the calculation of the left and right-side QDFTs by the above equations is effective. The inverse two-side 2-D ODFT is calculated by the similar formula

$$o_{n,m} = \sum_{p=0}^{N-1} W_{\mu_1}^{-np} \left(\sum_{s=0}^{M-1} O_{p,s} W_{\mu_2}^{-ms} \right), \tag{16}$$

when $n = 0 : (N-1)$ and $m = 0 : (M-1)$. We also can consider the following definition of the two-side 2-D ODFT:

$$O_{p,s} = \sum_{n=0}^{M-1} \left(\sum_{n=0}^{N-1} W_{\mu_1}^{np} o_{n,m} \right) W_{\mu_2}^{ms}. \tag{17}$$

For this transform, the column-row method can be used. Along each column (when m is fixed) the N-point left-side ODFT is calculated, and then along each row (when n is fixed) of the obtained data, the M-point right-side ODFT is calculated. Thus, since the operation of multiplication for octonions is not associative, the row-column and column-row two-side ODFTs are different. All above 2-D octonion transforms can be calculated by the 2-D QDFT, for which fast algorithms exist [1],[7]-[9],[23, 24].

Together with the two-side 2-D ODFT, the concepts of the right-side and left-side 2-D ODFTs can be used in imaging. Such one-side transforms can be effectively calculated not only by the row-column method, but with the concept of the tensor and paired representations, which were effectively applied for color and quaternion images [1, 37]-[41]. The tensor representation is effective for the prime size of the images and the paired for the case when the sizes are power of 2, prime, or even numbers. Such representation allow for reducing the calculation of the 2-D QDFTs to the calculation of the 1-D QDFTs over the splitting-signals which represent the image and can be used for image processing [27]-[36]. Therefore, the calculation of the 2-D QDFT as well as 2-D ODFT can be reduced to separate calculation of the 1-D transforms, and application of transforms in color image enhancement [37]-[41], filtration [17, 42, 26, 42] and image reconstruction [43]-[55].

5. CONCLUSION

The two-dimension two-side octonion discrete Fourier transform (2-D ODFT) is described in the octonion algebra. This transform can also be used in different models of gray-scale image representation in the octonion space. The calculation of the two-side 2-D ODFT can be accomplished was shown by using the fast 1-D left and right-side quaternion discrete Fourier transforms with any quaternion exponential kernel, when calculating two 2-D two-side QDFTs which define the two-side 2-D ODFT.

[1] A.M. Grigoryan,S.S. Agaian, Practical Quaternion Imaging with MATLAB, SPIE Press, 2017.

[2] A.M. Grigoryan, S.S. Agaian, Retolling of color imaging in the quaternion algebra, MathS), 1, 3, pp. 23-39 (2014).

[3] S.J. Sangwine, Fourier transforms of colour images using quaternion, or hypercomplex, numbers, Electronics Letters, 32, 21, pp. 1979–1980 (1996).

[4] S.J. Sangwine, T.A. Ell, J.M. Blackledge, M.J. Turner, The discrete Fourier transform of a color image, Proc. Image Processing II MMAA, pp. 430–441 (2000).

[5] S.J. Sangwine, T.A. Ell, Hypercomplex Fourier transforms of color images, Proc. IEEE ICIP, 1, pp. 137-140 (2001).

[6] T.A. Ell, Quaternion-Fourier transforms for analysis of 2-dimensional linear time-invariant partial differential systems, Proc. IEEE CDC, 1-4, pp. 1830–1841 (1993).

[7] A.M. Grigoryan, S.S. Agaian, Tensor transform-based quaternion Fourier transform algorithm, IS, 320, pp. 62-74 (2015)

[8] A.M. Grigoryan, S.S. Agaian, 2-D Left-side quaternion discrete Fourier transform fast algorithms, Proc. IS&T, 2016 Electronic Imaging: Algorithms and Systems XIV, (2016).

[9] A.M. Grigoryan, S.S. Again, Tensor representation of color images and fast 2-D quaternion discrete Fourier transform, Proc. SPIE, 9399, Image Processing: Algorithms and Systems XIII, (2015).

[10] W.R. Hamilton, Lectures on quaternions: Containing a systematic statement of a new mathematical method, Dublin: Hodges and Smith (1853).

[11] W.R. Hamilton, Elements of Quaternions, Logmans, Green and Co., London (1866).

[12] I.L. Kantor, A.S. Solodovnikov, Hypercomplex Numbers, Nauka, Moskow (1973).

[13] E. Hitzer, Quaternion Fourier transform on quaternion fields and generalizations, Advances in Applied Clifford Algebras, 17, 3, pp. 497-517 (2007).

[14] R.C. Gonzalez, R.E. Woods, Digital Image Processing, 2nd Ed., Prentice Hall (2001).

[15] L. Rabiner, B. Gold, Theory and application of digital signal processing, Prentice-Hall Inc., (1975).

[16] S.S. Agaian, Advances and problems of the fast orthogonal transforms for signal-images processing applications (Part 1), Nauka, 3, pp. 146-215 (1990).

[17] A.M. Grigoryan, S.S. Agaian, Multidimensional discrete unitary transforms: Representation, partitioning and algorithms, Marcel Dekker Inc., New York (2003).

[18] A.M. Grigoryan, S.S. Agaian, Split manageable efficient algorithm for Fourier and Hadamard transforms, IEEE TSP, 48, 1, pp. 172-183 (2000).

[19] Y. Zhou, W. Cao, L. Liu, S. Agaian, C.L. P. Chen, Fast Fourier transform using matrix decomposition, IS, 291, pp. 172-183 (2015).
[20] Z. Yang, S.-I. Kamata, Hypercomplex polar Fourier analysis for color image, Proc. ICIP (2011).
[21] A. Greenblatt, C.M. Lopez, Sos S. Agaian, Quaternion neural networks applied to prostate cancer Gleason grading, Proc. SMC, pp. 1144–1149 (2013).
[22] A.M. Grigoryan, S.S. Agaian, Cell Phone Camera Color Medical Imaging via Fast Fourier Transform, pp. 33–76, in Mobile Imaging for Healthcare Applications, SPIE Press, 2016.
[23] A.M. Grigoryan, S.S. Agaian, Color Enhancement and Correction for Camera Cell Phone Medical Images Using Quaternion Tools, pp. 77–117, in Mobile Imaging for Healthcare Applications, SPIE Press, 2016.
[24] S.C. Pei, J.J. Ding, J.H. Chang, Efficient implementation of quaternion Fourier transform, convolution and correlation by 2-D complex FFT, IEEE TSP, 49, pp. 2783-2797 (2001).
[25] A.M. Grigoryan, J. Jenkinson, S.S. Agaian, Quaternion Fourier transform based alpha-rooting method for color image measurement and enhancement, Proc. SIGPRO, 109, pp. 269–289 (2015).
[26] A.M. Grigoryan and M.M. Grigoryan, Brief Notes in Advanced DSP: Fourier Analysis With MATLAB., CRC Press Taylor and Francis Group, 2009.
[27] A.M. Grigoryan, An algorithm of the two-dimensional Fourier transform, Izvestiya VUZov SSSR, Radioelectronica, 27, 10, pp. 52-57 (1984).
[28] A.M. Grigoryan, An optimal algorithm for computing the two-dimensional discrete Fourier transform, Izvestiya VUZ SSSR, Radioelectronica, 29, 12, pp. 20-25 (1986).
[29] A.M. Grigoryan, New algorithms for calculating discrete Fourier transforms, JVMMF, 26, 9, pp. 1407-1412 (1986).
[30] A.M. Grigoryan, M.M. Grigoryan, Two-dimensional Fourier transform in the tensor presentation and new orthogonal functions, Avtometria, 1, pp. 21-27 (1986).
[31] A.M. Grigoryan, An algorithm for computing the two-dimensional Fourier transform of equal orders, Proc. IX All-Union Conference on CTI, 2, pp. 49-52 (1988).
[32] A.M. Grigoryan, An algorithm for computing the discrete Fourier transform with arbitrary orders, JVMMF, 30, 10, pp. 1576-1581 (1991).
[33] A.M. Grigoryan, 2-D and 1-D multi-paired transforms: Frequency-time type wavelets, IEEE TSP, 49, 2, pp. 344–353 (2001).
[34] A.M. Grigoryan, Fourier transform representation by frequency-time wavelets, IEEE TSP, 53, 7, pp. 2489-2497 (2005).
[35] A.M. Grigoryan, Multidimensional Discrete Unitary Transforms, chapter 19 (69 pages), Third Edition Transforms and Applications Handbook in The Electrical Engineering Handbook Series CRC Press, Taylor and Francis Group, January 11, 2010.
[36] A.M. Grigoryan, K. Naghdali, On a method of paired representation: Enhancement and decomposition by series direction images, JMIV, 34, 2, pp. 185–199 (2009).
[37] A.M. Grigoryan, S.S. Agaian, Alpha-rooting method of color image enhancement by discrete quaternion Fourier transform, Proc. SPIE 9019, Image Processing: Algorithms and Systems XII, pg. 12 (2014)
[38] S.S. Agaian, K. Panetta, A.M. Grigoryan, A new measure of image enhancement, Proc. IASTED, pp. 19-22 (2000).
[39] S.S. Agaian, K. Panetta, A.M. Grigoryan, Transform-based image enhancement algorithms, IEEE TIP, 10, 3, pp. 367–382 (2001).
[40] A.M. Grigoryan, S.S. Agaian, Transform-based image enhancement algorithms with performance measure, Advances in Imaging and Electron Physics, Academic Press, 130, pp. 165–242 (2004).
[41] F.T. Arslan, A.M. Grigoryan, Fast splitting α-rooting method of image enhancement: Tensor representation, IEEE Trans. on Image Processing, 15, 11, pp. 3375–3384 (2006).
[42] A.M. Grigoryan, E.R. Dougherty, S.S. Agaian, Optimal Wiener and Homomorphic Filtration: Review, SP, 121, pp. 111–138 (2016)
[43] A.M. Grigoryan, Solution of the problem on image reconstruction in computed tomography, JMIV, 54, 1, pp. 35–63 (2016).
[44] A.M. Grigoryan, M.M. Grigoryan, Image processing: Tensor transform and discrete tomography with MATLAB, CRC Press Taylor and Francis Group, 2012.
[45] A.M. Grigoryan, Method of paired transforms for reconstruction of images from projections: Discrete model, IEEE TIP, 12, 9, pp. 985-994 (2003).
[46] A. Grigoryan, S. Agaian, Tensor form of image representation: enhancement by image-signals, Proc. IS&T/SPIE EIST, (2003).
[47] A.M. Grigoryan, N. Du, Novel tensor transform-based method of image reconstruction from limited-angle projection data, Proc. SPIE, EI: Computational Imaging XII, pg. 12, (2014).
[48] F.T. Arslan, J.M. Moreno, and A.M. Grigoryan, Paired directional transform-based methods of image enhancement, Proc. SPIE, Visual Information Processing XV, 6246 (2006).
[49] F.T. Arslan, A.K. Chan, and A.M. Grigoryan, Directional denoising of aerial images by splitting-signals, Proc. IEEE TPS, (2006).
[50] F.T. Arslan and A.M. Grigoryan, Enhancement of medical images by the paired transform, Proc. IEEE ICIP, 1, pp. 537–540 (2007).
[51] A.M. Grigoryan, Nan Du, 2-D images in frequency-time representation: Direction images and resolution map, JEI, 19, 3, pg. 12 (2010).
[52] A.M. Grigoryan and Nan Du, Principle of superposition by direction images, IEEE Trans. IP, 20, 9, pp. 2531–2541 (2011).
[53] A.M. Grigoryan, Image reconstruction from finite number of projections: Method of transferring geometry, IEEE TIP, 22, 12, pp. 4738–4751 (2013).
[54] A.M. Grigoryan, Another Step towards Successful Tomographic Imaging in Cancer: Solving the Problem of Image Reconstruction, SPIE Press, pp. 295–338 (2014).
[55] A.M. Grigoryan, Comments on The discrete periodic Radon transform , IEEE Trans. SP, 58, 11, pp. 5962-5963 (2010).

Artyom Grigoryan *received his PhD in mathematics and physics from the Yerevan State University, Armenia, USSR. He is Associate Professor Department of Electrical Engineering, University of Texas at San Antonio. He is the author of 4 books, 2 patents, and many journal papers and specializing in the theory and application of Fourier transforms, image filtration and enhancement, quaternion imaging, and computerized tomography.*

Sos Agaian *received his PhD in mathematics and physics from the Steklov Institute of Mathematics, Russian Academy of Sciences. He is Professor of Electrical and Computer Engineering at the University of Texas, San Antonio. He has authored more than 500 scientific papers, 8 books, and holds 14 patents. Dr. Agaian is a Fellow of the SPIE, IS&T, AAAS, and IEEE.*